Tetrahedron 70 (2014) 4232–4244

Contents lists available at ScienceDirect

Tetrahedron

journal homepage: www.elsevier.com/locate/tet

An analysis of the influences dictating regioselectivity in platinum-catalyzed hydrosilylations of internal alkynes

Douglas A. Rooke, Zachary A. Menard, Eric M. Ferreira *

Department of Chemistry, Colorado State University, Fort Collins, CO 80523, United States

ARTICLE INFO

Article history:
Received 16 January 2014
Received in revised form 1 March 2014
Accepted 4 March 2014
Available online 13 March 2014

Keywords:
Hydrosilylation
Alkyne
Catalysis
Platinum
Regioselectivity

ABSTRACT

A full account of our studies on internal alkyne hydrosilylations using platinum catalysis is described. We demonstrate that these transformations are highly governed by the electronic characteristics of the alkyne substituents, wherein the hydride will add preferentially to the more electron-deficient alkyne carbon. The steric and coordinative capabilities of the substituents influence the selectivity to a much lesser extent, with propargylic alcohols a lone exception. The choice of silane is relevant in some cases; specific silanes will afford high regioselectivities while others are much less selective. Ultimately, the regioselectivity of addition can be quite predictable using ^{13}C NMR chemical shift data, allowing this reactivity to be incorporated into purposeful reaction design.

1. Introduction

The metal-catalyzed hydrosilylation reaction of alkenes and alkynes is a well-studied transformation.[1] Vinylsilanes, the products of alkyne hydrosilylation, can serve as useful precursors for Tamao–Fleming oxidations,[2] nucleophilic additions,[3] Hiyama couplings,[4] and halodesilylation reactions.[5] The widespread synthetic use of vinylsilanes rests upon the ability for their syntheses to be facile with high regio- and stereocontrol. An overwhelming majority of research on alkyne hydrosilylation has focused on the anti-Markovnikov addition of a silane across a terminal alkyne, a transformation that has reliably provided the terminal silane. Conversely, internal alkynes have received considerably less attention, which can be at least partially attributed to the difficulty of achieving regioselective transformations with this substrate class (Fig. 1).

Our entry into the field of metal-catalyzed hydrosilylations began with our desire to obtain (*E*)-α-silylenones, the geometric isomers of the products of our platinum catalyzed 1,2-silyl migration reaction of α-hydroxypropargylsilanes.[6] To our delight, this class of internal alkyne substrates afforded excellent regio- and stereoselectivity in catalytic hydrosilylation. We sought to fully understand the effects that influenced this process and its characteristic selectivity, and we previously reported several aspects our findings.[7] Herein, we present a comprehensive account of our study, illustrating how regioselective hydrosilylations of internal alkynes can be accomplished depending on the nature of the two alkyne substituents.

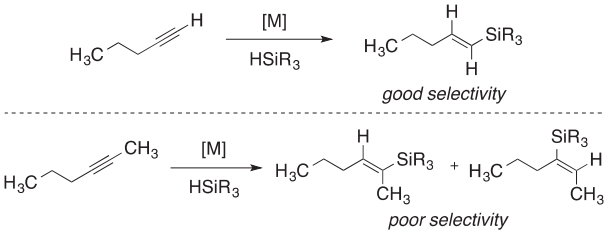

Fig. 1. Contrasting hydrosilylations of terminal and internal alkynes.

1.1. Background

There are many different methods reported to afford hydrosilylation products. However, the selectivity of Si–H addition can be a limitation of further synthetic utility for these methods. Radically induced hydrosilylation requires a silane that can easily undergo homolytic cleavage of the Si–H bond (Eq. 1).[8] The intermediate vinyl radical of this silane addition can be configurationally labile. High stereoselectivities have been achieved in certain cases, but for others the process is less effective. Lewis acids like $AlCl_3$ can

* Corresponding author. Tel.: +1 970 491 6379; fax: +1 970 491 1801; e-mail addresses: emferr@mail.colostate.edu, eric.ferreira@colostate.edu (E.M. Ferreira).

0040-4020/$ – see front matter © 2014 Elsevier Ltd. All rights reserved.
http://dx.doi.org/10.1016/j.tet.2014.03.012

catalyze the trans addition of a hydrosilane across an alkyne (e.g., Eq. 2).[9]

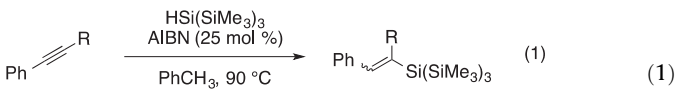

(1)

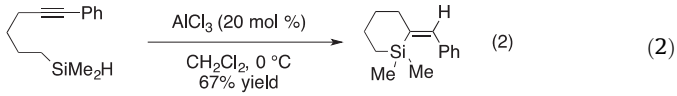

(2)

The strong Lewis acids that promote this transformation, however, can also catalyze the isomerization of the alkene. Early transition metal complexes, such as titanocene[10] and organoyttrium compounds[11] have been shown to catalyze the cis-addition of a silane across an alkyne. Due to issues primarily related to regioselectivity and functional group tolerance, the abovementioned methods of hydrosilylation have received little attention in the context of synthetic utility. Conversely, late transition metals have been the primary focus of research in regard to hydrosilylation.

The hydrosilylation chemistry catalyzed by late transition metals is both diverse and well-documented. Two separate mechanisms are cited for the observed regioselectivity of the hydrosilylation. One mechanism (the Crabtree–Ojima mechanism) has been observed in several cases using late transition metal catalysts based on Rh, Ir, and Ru.[12] This mechanism proceeds via a metallocarbene species, which leads to possible *E*/*Z* isomerizations. An exceptional catalytic system based on this mechanism, Trost and Ball have shown that $CpRu(MeCN)_3PF_6$ catalyzes an exclusively trans addition of silane with excellent selectivity and for a wide variety of internal alkynes (Eq. 3).[13]

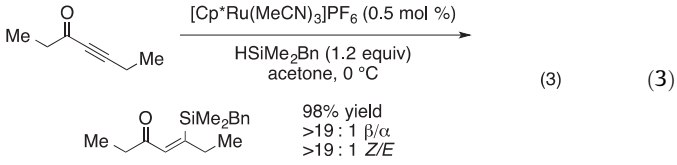

(3)

Pt-catalyzed hydrosilylations, alternatively, generally proceed though the standard Chalk–Harrod mechanism,[14] which provides complementary *syn*-addition products. Platinum and palladium catalysts are widely used for these hydrosilylation reactions and generally give products arising from the cis-addition of silane across an alkyne. In 1957, Speier was the first to report platinum-catalyzed hydrosilylations using H_2PtCl_6 (now termed Speier's Catalyst).[15] Today this catalyst is one of the most commonly used hydrosilylation catalysts in an industrial setting. The cis selectivity of addition is reflective of the Chalk–Harrod mechanism for Pt hydrosilylation (Fig. 2), wherein Pt(II) coordinates to an olefin (later applied to alkynes), and oxidative addition of the silane occurs. The resulting Pt(IV) complex undergoes migratory insertion across an olefin or alkyne, delivering a hydride to one of the two carbons. The resulting C–Pt–Si complex can then undergo reductive elimination to afford the cis hydrosilylation products.

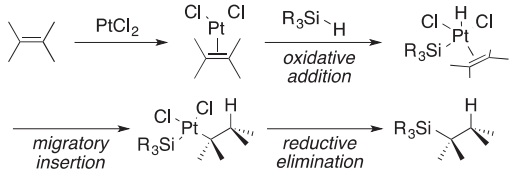

Fig. 2. The Chalk–Harrod mechanism for metal-catalyzed hydrosilylation.

The Chalk–Harrod mechanism has been widely accepted and can generally be applied to platinum-based hydrosilylation reactions. However, a number of phenomena are still unexplained by this mechanism. First, the other widely used catalyst in hydrosilylation is Karstedt's catalyst, a Pt(0)–divinyldisiloxane complex, which may implicate a similar catalytic mechanism invoking Pt(0) and Pt(II) oxidation states.[16] Second, it has been shown that alternative operational platinum catalysts, such as $Pt(cod)Cl_2$, are not active but instead are precatalysts that must undergo an induction period. Roy and Taylor have studied this induction period in depth and have concluded that the classical Chalk–Harrod mechanism can proceed through both Pt(II)–Pt(IV) and Pt(0)–Pt(II) catalytic cycles.[17] As long as the Chalk–Harrod mechanism holds, we can presume that the hydride is delivered during the migratory insertion step, and this step is thus playing a significant role in determining the regioselectivity and stereoselectivity of the net hydrosilylation.

Today, regioselective hydrosilylation on internal alkynes remains difficult, and research efforts have often focused on exploiting sterics dictated by both the substrate and catalyst system. Markó and co-workers have performed extensive work on the hydrosilylation of alkynes using bulky Pt/NHC catalysts developed in their lab.[18] Although chiefly focused on terminal alkynes, a number of internal alkynes were also investigated with some providing high regioselectivities. In 2011, Cook developed an active catalytic system for the hydrosilylation of propargylic alcohols.[19] Predictably, terminal alkynes showed excellent selectivity, while internal alkynes were much less selective unless significant steric bulk was employed to influence the addition. A recent report from Hosoya and co-workers illustrates Pd-catalyzed hydrosilylations of electron-deficient alkynes, where high regioselectivities have been achieved.[20] There have also been a few isolated examples where the alkyne electronic influence has been observed, often in substrate syntheses or specialized cases.[21]

The notion that electronic effects can dictate alkyne hydrosilylation was introduced by Tsipis in 1980. He hypothesized that the polarization of an alkyne would direct the hydride addition to the more electropositive carbon.[22] Up until this point, since most hydrosilylation centered around terminal alkynes and alkenes, sterics were believed to be the single most contributing factor affecting regioselectivity. Tsipis noted that the magnitude of difference in ^{13}C chemical shifts for terminal alkynes is rather large ($\sim$15–20 ppm).[23] However, for internal alkynes, the difference in alkyne chemical shifts is markedly less (approximately 3–5 ppm). These data could serve as predictors for which alkyne carbon has the lowest lying LUMO. He therefore posited that the hydrosilylation regioselectivity was impacted by this polarization in addition to the steric effects (Fig. 3).

Alami and co-workers, in their investigations of *ortho*-substituted arylacetylenes, showed one of the most salient first examples of highly selective internal alkyne hydrosilylation using PtO_2 (Fig. 4).[24] Interestingly, it was found that almost any substituent, from $-NO_2$ to $-i$-Pr, induced selectivity for the α-silyl isomer. This occurrence was observed even for cases involving diarylacetylenes—the silicon species will preferentially add to the alkyne carbon bearing the *ortho*-substituted aryl group.

More telling of the absolute electronic effects of this silane addition were their analyses of *para*-substituted diarylacetylenes (Fig. 5). Both alkyne carbons of these diarylacetylenes should have similar steric environments, and the *para*-substituent should exert a negligible coordinative effect. Therefore, any addition selectivity would likely be a consequence of alkyne polarization. In comparing

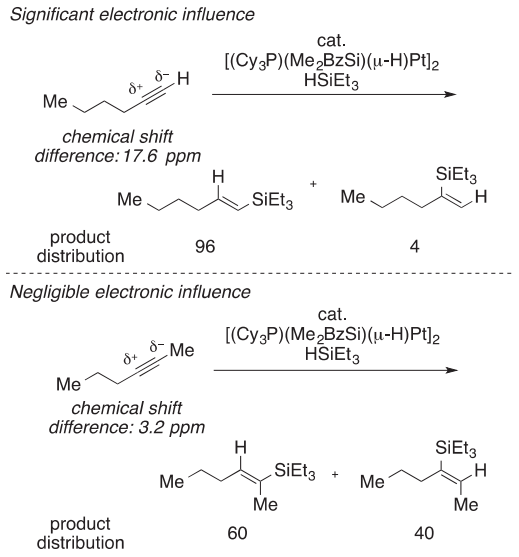

Fig. 3. Tsipis's proposal for electronic effects in alkyne hydrosilylation.

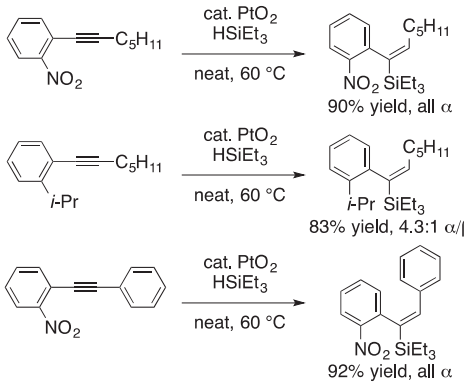

Fig. 4. Alami's hydrosilylations of aryl and diarylacetylenes.

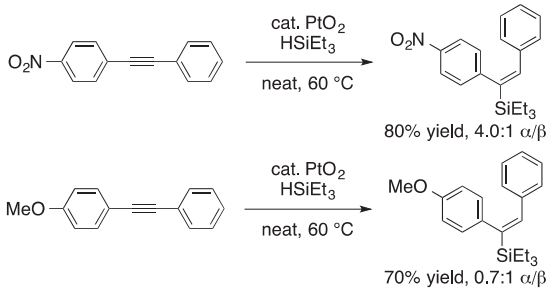

Fig. 5. Alami's hydrosilylations of *para*-substituted diarylacetylenes.

the depicted hydrosilylations, it is apparent that the electron-withdrawing *para*-nitrophenyl group induces α-silyl selectivity, whereas the electron-donating *para*-methoxyphenyl reverses selectivity to give the β-silyl isomer predominantly.

These observations integrate well into Tsipis's original hypothesis that the silylplatinum hydride will undergo migratory insertion across an alkyne, preferentially delivering the hydride to the more electropositive carbon. The Chalk–Harrod mechanism for Pt-catalyzed hydrosilylations can be readily applied to this concept, and selectivity distributions for the α and β isomers of a vinylsilane can ultimately be governed by the polarization of the alkyne (Fig. 6). In spite of these findings, it has still been generally regarded that

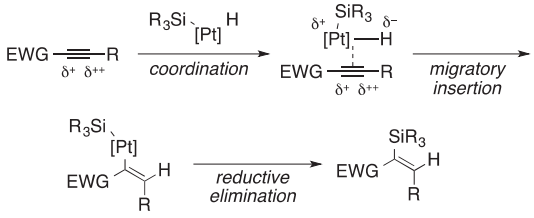

Fig. 6. Potential generalization of internal alkyne hydrosilylation based on electronic induction.

regioselectivity is difficult to control in many cases; given the synthetic utility of vinylsilanes, we sought to comprehensively evaluate this transformation to develop a full understanding of how this method can be properly exploited in synthetic contexts.

2. Results and discussion

2.1. Alkyne hydrosilylation—conditions and scope of electronic effects

As previously mentioned, we entered the field of hydrosilylation to selectively make (*E*)-silylenones as a complement to our 1,2-silicon migration method that affords (*Z*)-silylenones.[6] We envisioned that the highly polarized ynone substrates would induce high selectivity for the desired α-silyl regioisomer. To our delight, treatment of various ynones and trialkylsilanes with catalytic $PtCl_2$ proceeded under mild conditions to afford α-silylenones with generally excellent yields and selectivities (Table 1).[25] Even the hydrosilylation

Table 1
Pt-catalyzed hydrosilylations of ynones

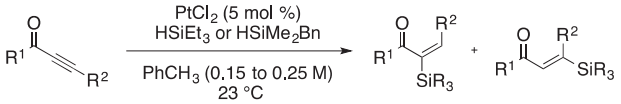

Entry	Substrate	Major product	Time (h)	Yield (%) α/β[a]
1	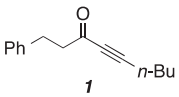 **1**	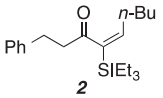 **2**	1.5	98 >19:1
2	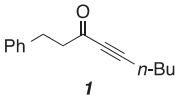 **1**	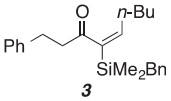 **3**	1.5	99 >19:1
3	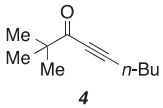 **4**	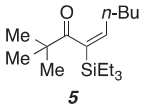 **5**	9	65 >19:1
4	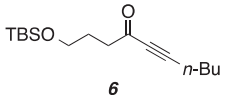 **6**	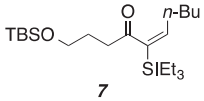 **7**	2	92 >19:1
5	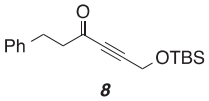 **8**	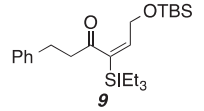 **9**	2	87 2:1

[a] Isolated yield; α/β ratio determined by ^{1}H NMR.

of highly hindered pivaloyl alkyne **4** afforded >19:1 regioselectivity for the α-silylenone, albeit in a more moderate yield.

One of the abovementioned substrates, the hydrosilylation of propargyl silyl ether **8** showed only slight preference for the α-silyl regioisomer (entry 5). We originally attributed this to the ethereal group coordinating to the silylplatinum intermediate, the inductive effect of the oxygenation, or some combination of these effects. Nonetheless, our interest was piqued, and we sought to elucidate this method as a useful, facile means to access stereodefined trisubstituted vinylsilanes.

Based on the high levels of regioselectivity observed in the hydrosilylations of ynones, we anticipated that other carbonyl-based electron-withdrawing groups, such as esters and amides would induce comparable reactivities and selectivities. To probe this hypothesis, a number of alkynes were subjected to conditions similar to our hydrosilylations of ynones (Table 2), with the salient difference being that CH_2Cl_2 was found to be a generally better solvent than $PhCH_3$.[26] All substrates, with the exception of aldehyde **24**, reacted efficiently, and the resulting products were isolated in high yields. Also notably, in all cases the hydrosilylations proceeded with high selectivity favoring the α-silyl isomer. Linear esters **10** and **12** provided >19:1 and 16:1 α/β selectivity, respectively, showing excellent differentiation over the *n*-butyl group. Branched esters **14** and **16** were unsurprisingly less regioselective, likely due to the increased steric bulk, affording still respectable 9.3:1 and 7.5:1 α/β selectivities. Weinreb (**18**) and phenyl (**20**) amides also demonstrated high selectivity. Even a carboxylic acid (**22**) was tolerated under the reaction conditions. The hydrosilylation of aldehyde **24** was the only observed outlier, affording a 58% yield in the best case and with varying regioselectivity (3.1–5.8:1). We attribute this outcome to differential carbonyl hydrosilylations of the product vinylsilanes. Competitive aldehyde hydrosilylation was consuming the product enals; differential reactivities of the α and β-isomers led to these variable results.

We also evaluated a number of methyl ynoate substrates by varying the other alkyne substituent and observing differences in regioselectivity of addition as well as in reactivity (Table 3). Increasing the size of this substituent (i.e., alkyne **26**) severely retarded the rate of reaction, yet still resulted in a 96% yield and >19:1 α/β selectivity (entry 2). More interestingly, substituents that

Table 2
Pt-catalyzed hydrosilylations of alkynes—various electron-withdrawing groups

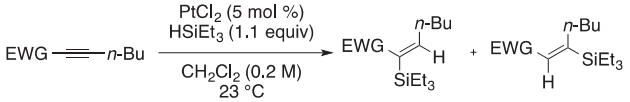

Entry	Substrate	Major product	Time (h)	Yield (%) α/β[a]
1	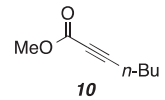 **10**	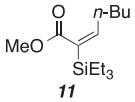 **11**	3	95 >19:1
2	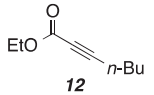 **12**	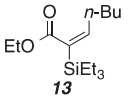 **13**	3	93 16:1
3	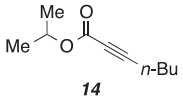 **14**	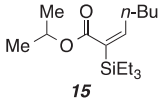 **15**	3	93 9.3:1
4	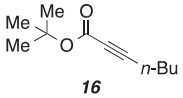 **16**	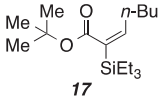 **17**	7	95 7.5:1
5	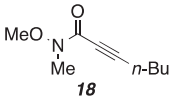 **18**	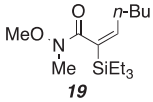 **19**	5	89 >19:1
6	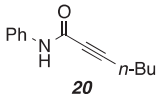 **20**	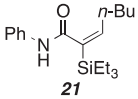 **21**	24	90 12:1
7	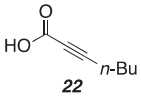 **22**	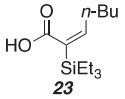 **23**	5.5	95 13:1
8	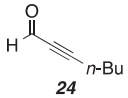 **24**	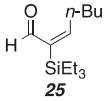 **25**	3	58 3.1–5.8:1

[a] Isolated yield; α/β ratio determined by ^{1}H NMR.

Table 3
Pt-catalyzed hydrosilylations of ynoates—varying the β-substituent

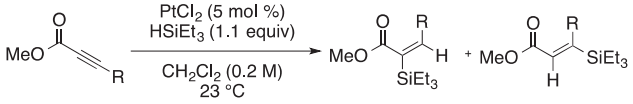

Entry	Substrate	Major product	Time (h)	Yield (%) α/β[a]
1	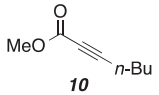 **10**	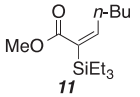 **11**	3	95 >19:1
2	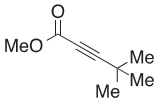 **26**	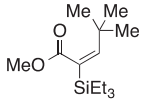 **27**	150	96 >19:1
3	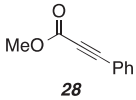 **28**	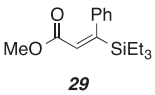 **29**	11	90 1:3.5
4	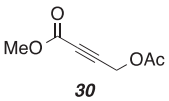 **30**	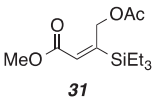 **31**	7	97 1:1.1
5	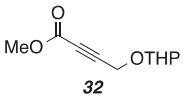 **32**	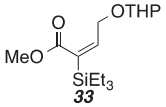 **33**	12	92 3.5:1
6	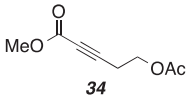 **34**	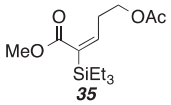 **35**	3	88 5.2:1

[a] Isolated yield; α/β ratio determined by ^{1}H NMR.

affected the polarization of the alkyne showed dramatically reduced hydrosilylation selectivity. Upon treatment of phenyl-substituted methyl ynoate **28** with $PtCl_2$ and $HSiEt_3$, the major product was the β-silyl regioisomer (1:3.5 α/β). Introducing oxygenation at the propargylic position similarly eroded selectivity, which had also been observed with ynone **8** (Table 1, entry 5). The reaction with propargylic acetate **30** also resulted in slight inversion of selectivity, affording a 1:1.1 α/β mixture of isomers. Diminished inductive effects can be observed in the hydrosilylation of homopropargylic acetate **34**. We anticipated that an additional methylene unit between the alkyne and the acetate group would decrease the inductive electronic effect of the acetate as well as reduce the possibility of coordination to the silylplatinum intermediate. Indeed, this substrate gave a higher regioselectivity, 5.2:1 α/β.

A number of commercially available Pt catalysts can be used for these hydrosilylation reactions with comparable outcomes. These catalysts were tested on substrate **10** in a series of similar condition sets with reasonable amounts of catalyst loadings (Scheme 1).

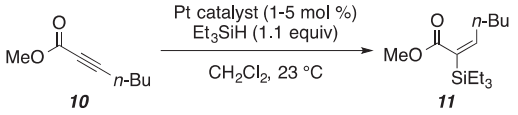

10 **11**

Catalyst, Time	Yield (%)	α : β
5 mol % $PtCl_2$, 3 h	98	>19.0 : 1
2.5 mol % $[(C_2H_4)PtCl_2]_2$, 5 h	99	>19.0 : 1
1 mol % Pt(dvds), 4 h	98	9.8 : 1

Scheme 1. Pt catalyst evaluation in hydrosilylation of ynoate **10**.

Reactions with both $PtCl_2$ (5 mol %) and Zeise's dimer $[\{(C_2H_4)PtCl_2\}_2]$ (5 mol % Pt) were essentially identical and showed exquisite selectivity for the α-isomer. Karstedt's catalyst [Pt(dvds)] (1 mol %)[27] was competent in the hydrosilylation, showing similarly high yields for enoate **11** but with somewhat diminished selectivity (9.8:1 α/β).

The hydrosilylation of internal alkynes can also be performed with remarkably low catalyst loadings (Scheme 2). The high solubility and activity of $[\{(C_2H_4)PtCl_2\}_2]$ in CH_2Cl_2 made it an ideal choice for a low catalyst loading reaction. For example, the hydrosilylation of alkyne **10** using 0.01 mol % catalyst effected the transformation to vinylsilane **11** in high yield and regioselectivity.[28]

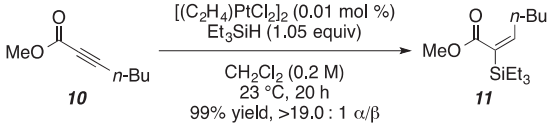

10 **11**

Scheme 2. Hydrosilylation of ynoate **10**—low catalyst loading.

After evaluating the effects of carbonyl-based electron-withdrawing groups as well as the different alkyne substituents, we felt it prudent to investigate different silanes as a third possible arm of substrate control. Simple, vinyltrialkylsilanes are inherently useful for due to their high stability; however, often a more activated silicon species is generally necessary for more general synthetic utility. Reactions, such as the Tamao–Fleming oxidation allow for vinylsilanes to serve as stable, masked carbonyls that can be unveiled later in a synthesis.[2] These C–Si bond oxidations primarily require halogen-, oxygen-, or aryl-substituted silicon species. The Hiyama–Denmark coupling represents another important utilization of the C–Si bond;[29] this transformation generally requires an activated silicon intermediate (i.e., not a simple trialkylsilane). For these reactions, the vinylsilane must again contain oxygenation, halogenation, or a surrogate carbon-based species that can generate this oxygenation or halogenation in situ. Consequently, methods for the selective installation of these aforementioned silicon groups would ideally lead to more general application in synthesis.

Thus, a number of different commercially available silanes, possessing various silane substituents, were tested with methyl heptynoate. As can be seen in Table 4, the yields for the transformations were consistently good. Even sterically large silanes (e.g., HSi(*t*-Bu)Me_2, entry 2) were competent reactants, albeit appreciably slower. For the silanes with carbon-based substituents (entries 1–6), there appeared to be a slight but observable electronic trend. Silanes bearing substituents capable of inductively withdrawing electron density (e.g., allyl, phenyl) appeared to erode the regioselectivity of the addition. In particular, $HSiPh_3$ provided a much lower regioselectivity (entry 6, 6.0:1 α/β). One potential rationalization is that the H–Pt–Si intermediate is less hydridic than ones with standard trialkylsilanes, possessing more anionic character on the silicon atom. The lessened hydridic nature of this species would consequently be less susceptible to the electronic influences dictating the alkyne insertion step.

For the alkoxysilanes evaluated (entries 7–10), there was no discernibly clear trend in regioselection. The regioselectivities were generally lower than the examples using trialkylsilanes, which may be reflective of a similarly diminished hydridic nature as in the $HSiPh_3$ case. The difference between triethoxysilane and trimethoxysilane, however, cannot be explained solely by this effect, and more subtle influences are clearly dictating this reactivity. Gratifyingly, 1,1,1,3,5,5,5-heptamethyltrisiloxane ($HSi(OTMS)_2Me$) was quite effective in providing similar regioselectivities (entry 10).[30] Vinylsilanes based on these species were subsequently found to be efficient participants in both halodesilylations and Hiyama–Denmark cross couplings.[7,31]

To further evaluate the influence of various silane reagents on regioselectivity, we tested six different silanes with a significantly less electronically-differentiated system (Table 5). The hydrosilylation of homopropargylic acetate **45** with triethylsilane gives a 3.8:1 selectivity for vinylsilane **46** (entry 1). In noticeable contrast to the hydrosilylations of methyl heptynoate (**10**), where regioselectivity was impacted by silane substitution, all six different silanes effected a relatively similar regioselective outcome in this case.

In the cases of ynone internal alkyne hydrosilylation, it was observed that propargylic oxygenation had a pronounced effect on the reaction regioselectivity (vide supra, **8**→**9**). More noticeably, the hydrosilylation of propargylic acetate **30** afforded a reversal of regioselectivity, favoring the β-silyl product relative to the methyl ester. Because of the apparent influence of propargylic oxygenation, we sought to investigate whether these functionalities could steer regioselectivity relative to other moieties. As an initial set of experiments, secondary propargylic alcohol **52** was protected as a trifluoroacetate (**53**), an acetate (**55**), and a triethylsilyl ether (**57**), and each alkyne was subjected to identical hydrosilylation conditions (Table 6). As illustrated, when the electron-withdrawing nature of the propargylic substituent is decreased, the regioselectivity of addition is lessened.

This trend was consistent with primary esters as well (Table 7). We subjected acetate protected 2-butyn-1-ol (**60**) to our hydrosilylation conditions, which only afforded modest selectivity (3.7:1) for the α-silyl isomer. Using the more electron withdrawing trifluoroacetate group (**62**), selectivity was greatly increased to a more synthetically useful 17:1 α/β ratio of isomers. To directly compare the influence of the two different propargyl acetates, protected diol

Table 4
Pt-catalyzed hydrosilylations of ynoate **10**—varying the silane

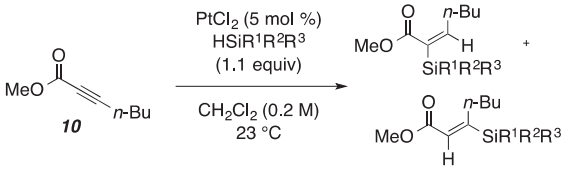

Entry	Silane	Major product	Time (h)	Yield (%) α/β[a]
1	$HSiEt_3$	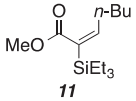 **11**	3	94 >19:1
2	$HSiMe_2t$-Bu	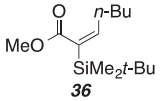 **36**	45	74 10:1
3	$HSiMe_2Bn$	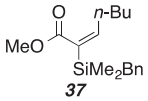 **37**	16	98 17.8:1
4	$HSiMe_2$(allyl)	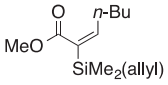 **38**	12	90 10.4:1
5	$HSiMe_2Ph$	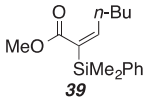 **39**	2	95 10.2:1
6	$HSiPh_3$	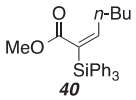 **40**	23	94 6.0:1
7	$HSiMe_2(OEt)$	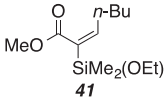 **41**	2	81 10.3:1
8	$HSi(OEt)_3$	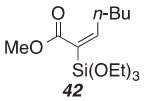 **42**	8	86 6.4:1
9	$HSi(OMe)_3$	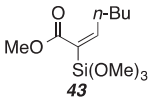 **43**	6.5	81 1.6:1
10[b]	$HSi(OTMS)_2Me$	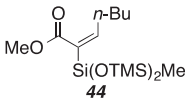 **44**	5	98 >19:1

[a] Isolated yield; α/β ratio determined by ^1H NMR.
[b] Using Pt(dvds) as catalyst.

64 was evaluated (entry 3) and the catalyst system was able to effectively differentiate both alkyne carbons (3.8:1 α/β), favoring silyl addition on the carbon proximal to the more electron deficient

Table 5
Pt-catalyzed hydrosilylations of alkyne **45**—varying the silane

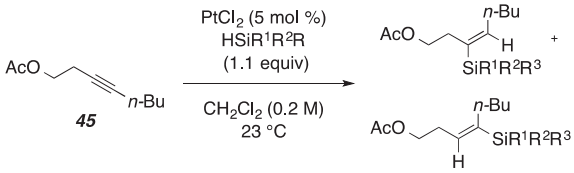

Entry	Silane	Major product	Time (h)	Yield (%) α/β[a]
1	$HSiEt_3$	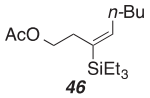 **46**	5.5	90 3.8:1
2	$HSiMe_2Ph$	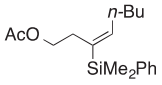 **47**	1.5	93 3.1:1
3	$HSiPh_3$	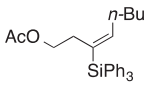 **48**	16	98 4.5:1
4	$HSiMe_2(OEt)$	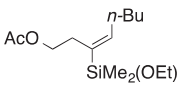 **49**	2.5	94 3.9:1
5	$HSi(OEt)_3$	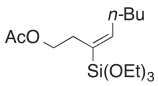 **50**	4	87 4.2:1
6	$HSi(OMe)_3$	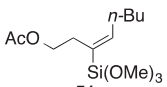 **51**	4.5	88 3.2:1

[a] Isolated yield; α/β ratio determined by ^1H NMR.

trifluoroacetate. This result also serves as evidence that coordination is not a significant contributor to regioselection, as the acetate should exert stronger coordinative influence on the catalyst than the trifluoroacetate, and it would therefore likely favor the observed minor product more appreciably.

2.2. Steric and coordination analysis

Taking into account all of these observations, it appeared clear that alkyne polarization plays the major role in dictating the hydrosilylation regioselectivity. Still, we wanted to evaluate if sterics and/or coordination were also influential.

To evaluate the influence of steric hindrance on hydrosilylation regioselectivity, we turned to all aliphatic alkyne substituents to eliminate any significant electronic or coordinative effects. First we subjected 5-decyne (**66**) to our hydrosilylation conditions (Scheme 3). The reaction proceeded in 3 h, a reaction time comparable to the aforementioned methyl heptynoate substrate (**10**). The reaction time for *tert*-butyl alkyne **68** was substantially longer (120 h), presumably reflecting the difficulty of coordination of the silyl–-platinum–hydride complex to the alkyne as well as the steric encumbrance during migratory insertion step.

Table 6
Pt-catalyzed hydrosilylations of substituted secondary propargylic alcohols

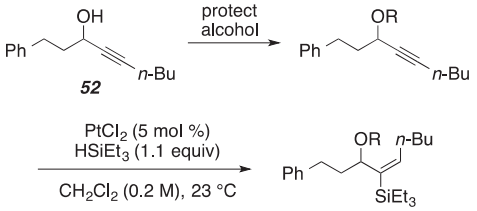

Entry	Substrate	Major product	Time (h)	Yield (%) α/β[a]
1	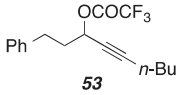	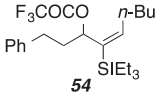	12	95 >19:1
2	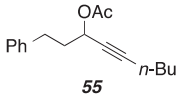	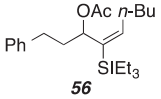	16	97 7.1:1
3	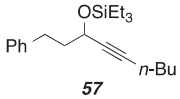	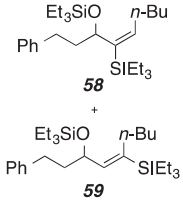	16	98 1.0:1

[a] Isolated yield; α/β ratio determined by ^{1}H NMR.

Table 7
Pt-catalyzed hydrosilylations of primary propargylic esters

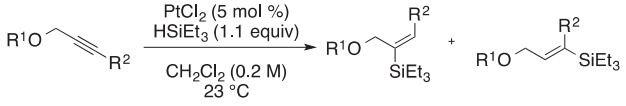

Entry	Substrate	Major product	Time (h)	Yield (%) α/β[a]
1	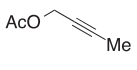	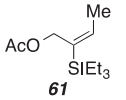	10	90 3.7:1
2	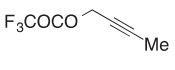	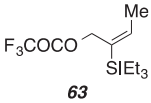	8	89 17:1
3	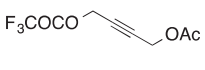	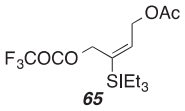	60	69 3.8:1

[a] Isolated yield; α/β ratio determined by ^{1}H NMR.

Interestingly, even though one side of alkyne **68** is significantly more hindered than the other, only a 1:2.2 α/β ratio of regioisomers is observed. This suggests that sterics may not be nearly as influential on the regioselectivity as the overall polarization of the alkyne. This premise is consistent with the hydrosilylations of the differentially substituted ynoates in Table 2 (entries 1–4). As the ester substituent increased in size, regioselectivity slightly but measurably decreased.

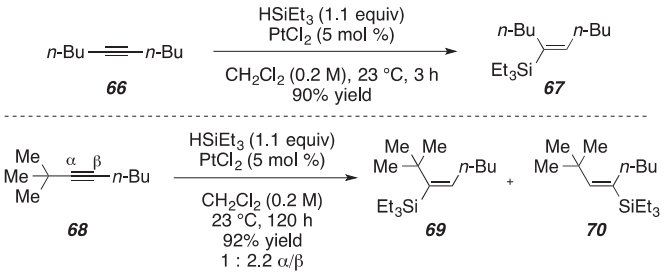

Scheme 3. Steric effects on Pt-catalyzed hydrosilylations.

The potential for catalyst coordination and its impact on regioselectivity also needed to be established. A recent example, Tomooka and co-workers employed a tethered, cleavable dimethylvinyl silyl directing group for the platinum-catalyzed hydrosilylation of alkynes (Fig. 7).[32] When the directing group was proximal, exquisite levels of regioselectivity were observed; as the distance between the alkyne and the directing group increased, however, the overall selectivity decreased accordingly.

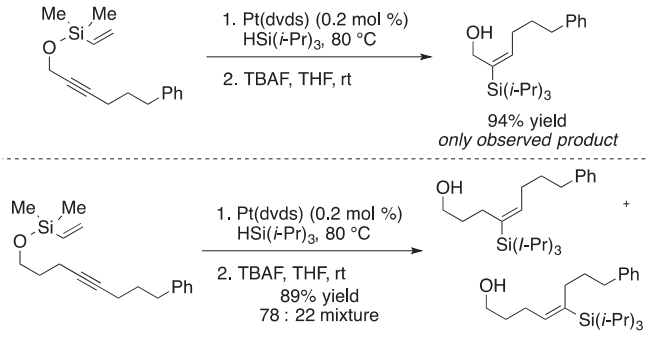

Fig. 7. Tomooka's internal alkyne hydrosilylation—alkene directing capability.

The hydrosilylations of a number of previously described substrates with propargylic oxygenation (e.g., **8**, **30**, **32**) displayed significantly diminished regioselectivity. Although these outcomes were consistent with solely electronic governance, we postulated that the proximal oxygen could also be influential via coordination of either the platinum or silicon atoms of intermediate **71**, and consequently direct silicon addition toward the side of said group (Fig. 8).

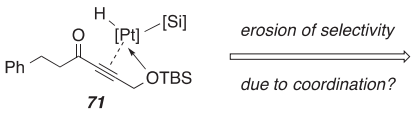

Fig. 8. The potential for regioselectivity via catalyst coordination.

To more definitively ascertain any potential effects of coordination on hydrosilylation regioselectivity, a primary propargylic alcohol was protected with groups of varying coordinative properties but similar inductive properties (Table 8). For example, we anticipated the methoxymethyl group (entry 1) would be more capable of catalyst coordination than a silyl ether (entry 3). These

Table 8
Pt-catalyzed hydrosilylations of protected propargylic alcohols

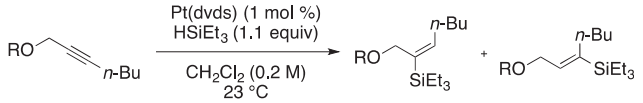

Entry	Substrate	Major product	Time (h)	Yield (%) α/β[a]
1	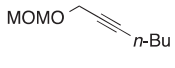 ***72***	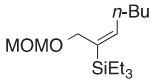 ***73***	16	73 2.8:1
2	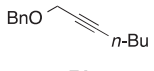 ***74***	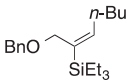 ***75***	16	96 3.2:1
3	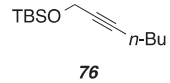 ***76***	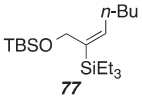 ***77***	16	78 2.7:1

[a] Isolated yield; α/β ratio determined by ^{1}H NMR.

substrates were then subjected to hydrosilylation conditions using Pt(dvds). As can be seen, very similar α/β product ratios were observed across all three substrates.

To further study the possibility of oxygen coordination influence of regioselectivity, an identical study was carried out with homopropargylic alcohol derivatives (Table 9).

Table 9
Pt-catalyzed hydrosilylations of protected homopropargylic alcohols

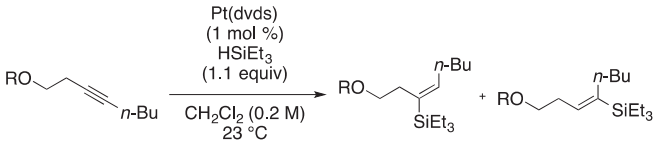

Entry	Substrate	Major product	Time (h)	Yield (%) α/β[a]
1	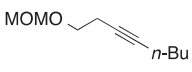 ***78***	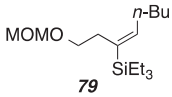 ***79***	16	93 2.1:1
2	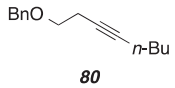 ***80***	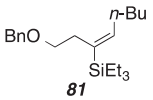 ***81***	16	98 2.0:1
3	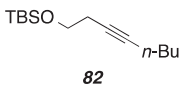 ***82***	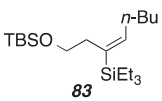 ***83***	16	95 1.9:1

[a] Isolated yield; α/β ratio determined by ^{1}H NMR.

The above tables perhaps best illustrate the lack of influence that coordinating groups have on hydrosilylation regioselectivity. Both the propargylic and the homopropargylic systems have essentially identical observed product ratios even though these ranges of substrates are likely to have different coordinative properties.

Alcohols themselves, however, showed a substantial capability for impacting regioselectivity, implicating a potential coordinative effect. Examples are illustrated in Table 10. Excellent selectivity was observed for the hydrosilylation of primary and secondary propargyl alcohols **52** and **85**; however, 2-butyn-1-ol (**87**) was curiously less selective. Sterics could potentially play a role with the relatively small methyl alkyne substituent.[21] Although highly hindered alkyne **89** showed moderate regioselectivity, similarly hindered, yet more significantly polarized alkyne **91** showed a much higher isomeric ratio (9.2:1 α/β). The effect of the alcohol functional group did not extend to homopropargylic systems; much lower regioselectivities were observed (entry 6).

Table 10
Pt-catalyzed alkyne hydrosilylations—the effect of alcohols

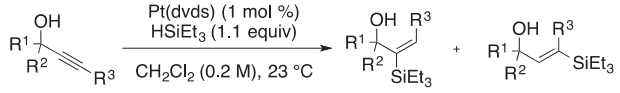

Entry	Substrate	Major product	Time (h)	Yield (%) α/β[a]
1	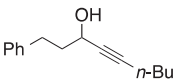 ***52***	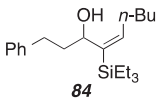 ***84***	3	86 >19:1
2	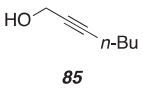 ***85***	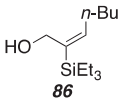 ***86***	5	92 >19:1
3	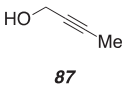 ***87***	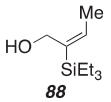 ***88***	24	97 3.3:1
4	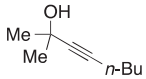 ***89***	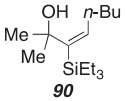 ***90***	24	88 3.2:1
5	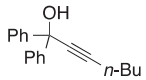 ***91***	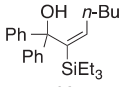 ***92***	24	81 9.2:1
6	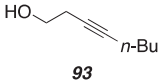 ***93***	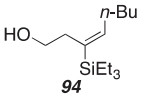 ***94***	6	97 3.0:1

[a] Isolated yield; α/β ratio determined by ^{1}H NMR.

The high regioselectivities observed in these propargylic alcohol hydrosilylations were intriguing. One could surmise that the alcohol may participate in a favorable hydrogen bond interaction with the catalytic platinum intermediate, thus acting as a directing group for the addition process. Our current hypothesis is that the *d*-electrons on the Pt center are engaging in this hydrogen bond (**95**, Fig. 9).[33]

An additional important observation was made during the studies of these propargylic alcohols and derivatives. In general, the

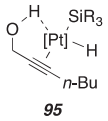

95

Fig. 9. Possible catalyst coordination mode for alcohol moieties.

three catalyst precursors we had been evaluating ($PtCl_2$, Zeise's dimer, and Pt(dvds)) behaved quite similarly across most substrates. The hydrosilylations of methyl heptynoate (Scheme 1) are indicative of this similarity. The propargylic alcohol substrates, however, afforded much lower yields than typically observed for hydrosilylations when $PtCl_2$ or Zeise's dimer were employed (Table 11). HCl, a potential byproduct of the Pt(II) salt catalyst induction period, may promote the decomposition of the product or starting material alcohols through ionization pathways. Pt(dvds) was able to circumvent the problem of acid generation affording excellent yield and selectivity (92% yield, >19:1 α/β) of the vinylsilane.

Table 11
Pt-catalyzed hydrosilylations of propargylic alcohols—effect of precatalyst

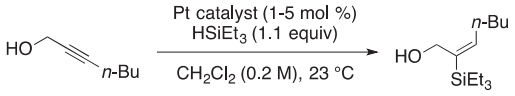

85 86

Entry	Catalyst	Time (h)	Yield (%) α/β
1	$PtCl_2$ (5 mol %)	6	45 >19:1
2	$[\{(C_2H_4)PtCl_2\}_2]$ (2.5 mol %)	4	47 >19:1
3	Pt(dvds) (1 mol %)	5	92 >19:1

2.3. Predictability in regioselection

Toward overall synthetic utility, we believed that it was important for this transformation to be as predictable as possible. Therefore, we were curious if the characteristic data of the alkyne substrates could lead to better predictability. A few isolated examples have employed ^{13}C NMR chemical shift data to differentiate alkyne carbons and rationalize hydrosilylation regioselectivity. Tsipis's seminal report, which hypothesized an electronic effect influencing selectivity, discussed such ^{13}C NMR data in the evaluation of a number of aliphatic alkynes.[22] Others have invoked the analysis of ^{13}C NMR data to explain the high regioselectivity for the hydrosilylation of terminal alkynes.[34] More recently, Alami and co-workers correlated ^{13}C NMR data to the regioselectivity of palladium-catalyzed hydrostannylations (Fig. 10), specifically focusing on the differences between *ortho*-substituted diarylacetylenes and their *para*-substituted counterparts.[35]

In this work, it was shown that the *para*-substituted phenyl diarylacetylenes featured relatively small differences in the α and β ^{13}C chemical shifts. The corresponding hydrostannylation regioselectivities were consistent with these differences. In contrast, the *ortho*-substituted systems possessed much greater chemical shift differences, and correlating larger regioselectivities were observed. A subsequent report by Gevorgyan and co-workers indicated that ^{13}C chemical shifts should not be applied with these *ortho*-substituted cases.[36] With this backdrop, we were eager to probe this concept to the internal alkyne hydrosilylations we had been investigating.

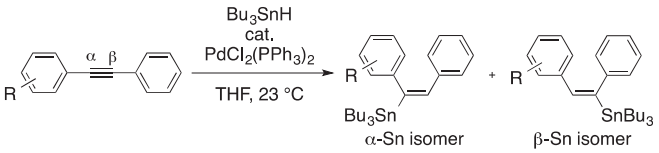

Entry	R	^{13}C Chemical Shifts δ(C_α)	δ(C_β)	$\Delta\delta_{C\beta-C\alpha}$	α : β
1	*p*-CHO	88.5	93.3	4.8	5.7 : 1
2	*p*-Me	89.6	88.7	-0.9	1.0 : 1
3	*p*-OMe	89.4	88.1	-1.3	0.7 : 1
4	*o*-CHO	84.9	96.3	11.4	>19 : 1
5	*o*-Me	88.6	93.6	5.0	13.3 : 1
6	*o*-OMe	85.7	93.4	7.7	9 : 1

Fig. 10. Alami's catalytic hydrostannylation of diarylacetylenes—correlation with ^{13}C NMR data.

As illustrated in Table 12, the hydrosilylations of select methyl ynoate substrates afforded sequentially decreasing regioselectivities even though the four respective substituents are of relatively similar size. An evaluation of alkyne ^{13}C chemical shifts for each compound clearly shows that each group exerts a noticeably different inductive effect.

Table 12
Pt-catalyzed ynoate hydrosilylations—correlation to ^{13}C NMR data

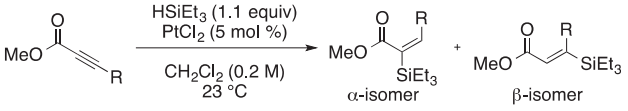

Entry	Substrate	^{13}C chemical shifts δ(Cα)	δ(Cβ)	Δδ(Cβ−Cα)	α/β[a]
1	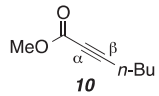 10	73.0	90.1	17.1	>19:1
2	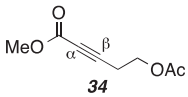 34	74.0	85.0	11.0	5.2:1
3	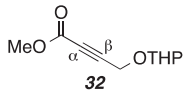 32	77.4	84.2	6.8	3.5:1
4	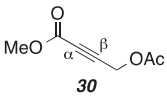 30	81.6	78.0	−3.6	0.9:1

[a] Determined by ^1H NMR.

The hydrosilylation of methyl heptynoate (**10**, entry 1) produces the enoate with high regioselectivity; this corresponds with a high difference in alkyne carbon chemical shifts (Δ=17.1 ppm). Homopropargylic acetate **34** shows markedly less α-selectivity, and accordingly the alkyne carbons are less differentiated (11.0 ppm). On the other end of the spectrum, a propargylic acetate moiety (i.e., alkyne **30**) seemingly exerts a stronger electronic influence than the methyl ester, showing a slight preference for the β-silyl regioisomer and a negative difference between δ(Cβ) and δ(Cα). Overall, the magnitude and direction of the difference between alkyne carbon chemical shifts directly corresponds to observed regioselectivity of hydrosilylation.

This correlation extended to the aforementioned alkynes featuring propargylic or homopropargylic oxygenation (Fig. 11). As

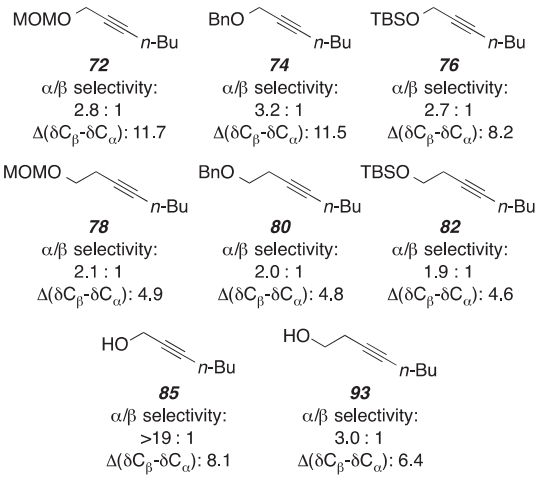

Fig. 11. ^{13}C NMR analysis of propargylic and homopropargylic alcohols and derivatives.

discussed, similar hydrosilylation regioselectivities were observed in both classes regardless of the potential coordinative abilities of the respective functional groups. In evaluating the ^{13}C NMR data, it was clear the correlation of this data and their related electronic implications were well aligned with the observed regioselection. These data also corroborated the lack of a coordinative effect for the compounds in Tables 8 and 9. Alternatively, this data also strongly implicates the directing impact of a propargylic alcohol (i.e., alkyne **85**), while indicating the absence of a similar effect for a homopropargylic alcohol.

Taking this information fully into account, the electronic effect in internal alkyne hydrosilylation should be able to be incorporated into purposeful reaction design. Table 13 highlights an example. Alcohol **96** can be protected with common groups that feature different electronic properties. The correlating inductive impact on the alkyne carbons can be readily measured by NMR. As evidenced, synthetically viable selectivity can be achieved in this hydrosilylation by the judicious choice of alcohol protecting group (i.e., the trifluoroacetate). This example illustrates how reasonable predictability can be achieved in future alkyne hydrosilylations.

3. Conclusion

In summary, the hydrosilylation of internal alkynes, once considered to be generally unselective, can be harnessed quite effectively using substrate control. We have demonstrated the hydrosilylations of numerous internal alkynes using mild conditions and simple, stable Pt catalysts. In many cases, these reactions proceed in high yield and selectivity. To further elucidate selectivity controls, the effects of electronics, steric hindrance, and coordination were comprehensively evaluated. Notably, it was found that alkyne polarization afforded the greatest influence over the regioselectivity of silane addition. This electronic effect can be reasonably quantified using ^{13}C NMR data. A greater magnitude between alkyne carbon chemical shifts correlates to greater observed regioselectivity of silane addition.[37] The effects of sterics are measurable but significantly less influential. Although proximal oxygen atoms could conceivably direct selectivity, after evaluation of numerous substrates it can be determined that the inductive effect of the oxygen group probably affects overall regioselectivity more so than coordination, with alcohols themselves providing an exception. This expansion of hydrosilylation methodology will hopefully serve the synthetic community with its ability to generate synthetically useful stereodefined trisubstituted alkenes.

Table 13
Pt-catalyzed alkyne hydrosilylations—protecting group strategy by correlation with ^{13}C NMR data

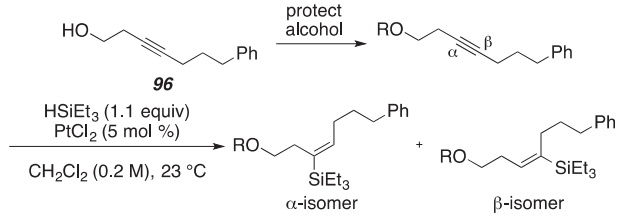

Entry	Substrate	^{13}C chemical shifts		Δδ(Cβ−Cα)	α/β[a]
		δ(Cα)	δ(Cβ)		
1	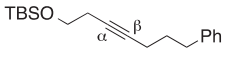 **97**	77.8	81.3	3.5	1.4:1
2	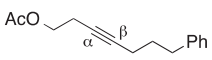 **98**	76.5	81.8	5.3	2.5:1
3	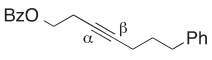 **99**	76.5	82.0	5.5	2.7:1
4	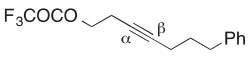 **100**	74.7	83.0	8.3	4.3:1 (76% isol. yield)

[a] Determined by ^{1}H NMR.

4. Experimental section

4.1. Materials and methods

Methylene chloride, tetrahydrofuran, ether, and toluene were purified by passing through activated alumina columns. All other reagents were used as received unless otherwise noted. Commercially available chemicals were purchased from Alfa Aesar (Ward Hill, MA), Sigma–Aldrich (St. Louis, MO), Gelest (Morrisville, PA), Oakwood Products (West Columbia, SC), Strem (Newburport, MA), and TCI America (Portland, OR). Qualitative TLC analysis was performed on 250 mm thick, 60 Å, glass backed, F_{254} silica (Silicycle, Quebec City, Canada). Visualization was accomplished with UV light and exposure to either *p*-anisaldehyde or $KMnO_4$ stain solutions followed by heating. Flash chromatography was performed using Silicycle silica gel (230–400 mesh). ^{1}H NMR spectra were acquired on either a Varian Mercury 300 (at 300 MHz), a Varian Inova 400 (at 400 MHz), or a Varian 400 MR (at 400 MHz) and are reported relative to $SiMe_4$ (δ 0.00). ^{13}C NMR spectra were acquired on either a Varian Inova 400 (at 100 MHz), a Varian Mercury 300 (at 75 MHz), or a Varian 400 MR (at 100 MHz) and are reported relative to $SiMe_4$ (δ 0.0). All IR spectra were obtained on NaCl plates (film) with a Bruker Tensor 27. High resolution mass spectrometry data were acquired by the Colorado State University Central Instrument Facility on an Agilent 6210 TOF LC/MS.

4.2. General procedure for Pt-catalyzed alkyne hydrosilylations

To a solution of the alkyne substrate and silane (1.1 equiv) in CH_2Cl_2 (0.2 M in substrate) was added $PtCl_2$ (5 mol %) under either argon or an ambient atmosphere. The reaction mixture was allowed to stir at room temperature until TLC indicated consumption of the starting material, at which point the reaction mixture was filtered through a small plug of silica gel, washing with Et_2O ($\sim$3$\times$ reaction volume). The solvent was removed by rotary evaporation, and the resulting residue was purified by flash chromatography to afford the vinylsilane. The crude reaction mixture was analyzed by ^{1}H NMR to determine the isomeric ratio prior to purification. Typically, the α and β isomers of the vinylsilanes were inseparable by flash column chromatography, although larger columns were sometimes effective at separation.

*4.2.1. Methyl (E)-2-(tert-butyldimethylsilyl)hept-2-enoate (**36**).* Hydrosilylation performed under Ar. Colorless oil. Yield 74%, 10.0:1 α/β. R_f=0.56 in 19:1 hexanes/Et_2O. IR (film) 2957, 1718, 1604, 1465, 1200, 835 cm^{-1}; ^{1}H NMR (400 MHz, $CDCl_3$) δ 6.07 (t, J=7.2 Hz, 1H), 3.71 (s, 3H), 2.26 (q, J=7.3 Hz, 2H), 1.45–1.28 (comp. m, 4H), 0.94–0.89 (comp. m, 12H), 0.11 (s, 6H); ^{13}C NMR (100 MHz, $CDCl_3$) δ 172.3, 151.2, 134.8, 51.5, 32.2, 31.7, 27.1, 22.8, 17.8, 14.4, −5.3; HRMS (APCI$^+$) m/z calcd for $(M+H)^+$ $[C_{14}H_{29}OSi]^+$: 257.1937, found 257.1917.

*4.2.2. Methyl (E)-2-(benzyldimethylsilyl)hept-2-enoate (**37**).* Hydrosilylation performed under air. Colorless oil. Yield 98%, 17.8:1 α/β. R_f=0.53 in 19:1 hexanes/Et_2O. IR (film) 2958, 1717, 1601, 1493, 1199 cm^{-1}; ^{1}H NMR (400 MHz, $CDCl_3$) δ 7.19 (t, J=7.5 Hz, 2H), 7.06 (t, J=7.4 Hz, 1H), 6.99 (d, J=6.9 Hz, 2H), 6.06 (t, J=7.2 Hz, 1H), 3.73 (s, 3H), 2.34 (q, J=7.3 Hz, 2H), 2.23 (s, 2H), 1.40–1.24 (comp. m, 4H), 0.89 (t, J=7.2 Hz, 3H), 0.09 (s, 6H); ^{13}C NMR (100 MHz, $CDCl_3$) δ 170.8, 153.9, 139.7, 133.7, 128.5, 128.4, 128.3, 128.2, 124.2, 51.2, 31.6, 31.2, 25.7, 22.5, 14.0, −3.4; HRMS (DART$^+$) m/z calcd for $(M+NH_4)^+$ $[C_{17}H_{30}NO_2Si]^+$: 308.2046, found 308.2040.

*4.2.3. Methyl (E)-2-(allyldimethylsilyl)hept-2-enoate (**38**).* Hydrosilylation performed under air. Colorless oil. Yield 90%, 10.4:1 α/β. R_f=0.41 in 19:1 hexanes/Et_2O. IR (film) 2958, 1718, 1433, 1250, 1199 cm^{-1}; ^{1}H NMR (400 MHz, $CDCl_3$) δ 6.18 (t, J=7.1 Hz, 1H), 5.74 (ddt, J=16.3, 10.5, 8.1 Hz, 1H), 4.86–4.82 (comp. m, 2H), 3.72 (s, 3H), 2.36 (q, J=7.2 Hz, 2H), 1.65 (d, J=8.0 Hz, 2H), 1.44–1.28 (comp. m, 4H), 0.90 (t, J=7.1 Hz, 3H), 0.12 (s, 6H); ^{13}C NMR (100 MHz, $CDCl_3$) δ 171.2, 153.7, 134.9, 134.5, 113.9, 51.5, 31.9, 31.7, 23.6, 22.8, 14.4, −3.1; HRMS (DART$^+$) m/z calcd for $(M+NH_4)^+$ $[C_{13}H_{28}NO_2Si]^+$: 258.1889, found 258.1884.

*4.2.4. Methyl (E)-2-(dimethyl(phenyl)silyl)hept-2-enoate (**39**).* Hydrosilylation performed under Ar. Colorless oil. Yield 95%, 10.2:1 α/β. R_f=0.29 in 19:1 hexanes/Et_2O. IR (film) 2957, 1717, 1606, 1200, 835 cm^{-1}; ^{1}H NMR (400 MHz, $CDCl_3$) δ 7.54–7.52 (comp. m, 2H), 7.37–7.34 (comp. m, 3H), 6.20 (t, J=7.2 Hz, 1H), 3.65 (s, 3H), 2.39 (q, J=7.3 Hz, 2H), 1.43–1.27 (comp. m, 4H), 0.89 (t, J=7.2 Hz, 3H), 0.42 (s, 6H); ^{13}C NMR (100 MHz, $CDCl_3$) δ 171.2, 155.4, 138.1, 134.60, 134.58, 129.7, 128.3, 51.6, 32.2, 31.7, 23.0, 14.5, −1.9; HRMS (APCI$^+$) m/z calcd for $(M+NH_4)^+$ $[C_{16}H_{28}NO_2Si]^+$: 294.1889, found 294.1888.

*4.2.5. Methyl (E)-2-(triphenylsilyl)hept-2-enoate (**40**) and methyl (E)-3-(triphenylsilyl)hept-2-enoate.* Hydrosilylation performed under Ar. Colorless oil. Yield 94%, 6.0:1 α/β. R_f=0.26 in 19:1 hexanes/Et_2O. *α-Isomer*: IR (film) 2955, 1715, 1485, 1203, 1109 cm^{-1}; ^{1}H NMR (400 MHz, $CDCl_3$) δ 7.58 (app. d, J=8.0 Hz, 6H), 7.45–7.36 (comp. m, 9H), 6.32 (t, J=7.3 Hz, 1H), 3.48 (s, 3H), 2.47 (q, J=7.3 Hz, 2H), 1.44–1.28 (comp. m, 4H), 0.90 (t, J=7.2 Hz, 3H); ^{13}C NMR (100 MHz, $CDCl_3$) δ 171.0, 158.9, 136.6, 134.1, 131.7, 130.0, 128.2, 51.5, 32.3, 31.5, 22.9, 14.3; HRMS (APCI$^+$) m/z calcd for $(M+NH_4)^+$ $[C_{26}H_{32}NO_2Si]^+$: 418.2202, found 418.2183. *β-Isomer*: IR (film) 3070, 2956, 1721, 1485, 1714, 700 cm^{-1}; ^{1}H NMR (400 MHz, $CDCl_3$) δ 7.58–7.56 (m, 6H), 7.48–7.38 (comp. m, 9H), 6.23 (s, 1H), 3.72 (s, 3H), 2.75 (app. t, J=7.5 Hz, 2H), 1.42–1.11 (comp. m, 4H), 0.67 (t, J=7.0 Hz, 3H); ^{13}C NMR (100 MHz, $CDCl_3$) δ 165.9, 161.6, 136.7, 133.0, 130.2, 128.3, 51.3, 32.2, 32.0, 23.3, 13.9; LRMS (ESI$^+$) m/z calcd for $(M+H)^+$ $[C_{26}H_{29}O_2Si]^+$: 401.2, found 401.2.

*4.2.6. Methyl (E)-2-(ethoxydimethylsilyl)hept-2-enoate (**41**).* Hydrosilylation performed under Ar. Colorless oil. Yield 81%, 10.3:1 α/β. R_f=0.52 in 9:1 hexanes/Et_2O. IR (film) 2960, 1719, 1252, 1199, 835 cm^{-1}; ^{1}H NMR (400 MHz, $CDCl_3$) δ 6.38 (t, J=7.2 Hz, 1H), 3.73 (s, 3H), 3.69 (q, J=7.0 Hz, 2H), 2.42 (q, J=7.3 Hz, 2H), 1.44 (quint, J=7.4 Hz, 2H), 1.34 (sextet, J=7.4 Hz, 2H), 1.19 (t, J=7.0 Hz, 3H), 0.91 (t, J=7.2 Hz, 3H), 0.25 (s, 6H); ^{13}C NMR (100 MHz, $CDCl_3$) δ 170.7, 155.1, 134.1, 59.0, 51.4, 31.6, 31.4, 22.7, 18.7, 14.2, −1.4.

*4.2.7. Methyl (E)-2-(triethoxysilyl)hept-2-enoate (**42**) and methyl (E)-3-(triethoxysilyl)hept-2-enoate.* Hydrosilylation performed under Ar. Colorless oil. Yield 86%, 6.4:1 α/β. R_f=0.35 in 9:1 hexanes/Et_2O (α-isomer), 0.43 in 9:1 hexanes/Et_2O (β-isomer). *α-Isomer*: IR (film) 2975, 1720, 1609, 1434, 1391, 1206, 788 cm^{-1}; ^{1}H NMR (400 MHz, $CDCl_3$) δ 6.68 (t, J=7.2 Hz, 1H), 3.84 (q, J=7.0 Hz, 6H), 3.73 (s, 3H), 2.46 (q, J=7.2 Hz, 2H), 1.43 (quint, J=7.4 Hz, 2H), 1.33 (sextet, J=7.4 Hz, 2H), 1.21 (t, J=7.0 Hz, 9H), 0.90 (t, J=6.9 Hz, 3H); ^{13}C NMR (100 MHz, $CDCl_3$) δ 169.8, 160.5, 127.5, 59.3, 51.7, 31.8, 31.4, 22.9, 18.6, 14.3; LRMS (ESI$^+$) m/z calcd for $(M+H)^+$ $[C_{14}H_{29}O_5Si]^+$: 305.2, found 305.2. *β-Isomer*: IR (film) 2976, 1727, 1434, 1082, 963, 783 cm^{-1}; ^{1}H NMR (400 MHz, $CDCl_3$) δ 6.31 (s, 1H), 3.84 (q, J=7.1 Hz, 6H), 3.72 (s, 3H), 2.67 (t, J=7.5 Hz, 2H), 1.50–1.33 (comp. m, 2H) 1.25 (t, J=7.0 Hz, 9H), 0.93 (t, J=7.2 Hz, 3H); ^{13}C NMR (100 MHz, $CDCl_3$) δ 166.3, 157.2, 130.1, 59.2, 51.5, 31.9, 31.1, 23.6, 18.6, 14.4; LRMS (ESI$^+$) m/z calcd for $(M+H)^+$ $[C_{14}H_{29}O_5Si]^+$: 305.2, found 305.2.

*4.2.8. Methyl (E)-2-(trimethoxysilyl)hept-2-enoate (**43**) and methyl (E)-3-(trimethoxysilyl)hept-2-enoate.* Hydrosilylation performed under Ar. Colorless oil. Yield 81%, 1.6:1 α/β. R_f=0.30 in 9:1 hexanes/EtOAc (α-isomer), 0.46 in 9:1 hexanes/Et_2O (β-isomer). *α-Isomer*: IR

(film) 2954, 2844, 1721, 1608, 1207 cm^{-1}; ^1H NMR (400 MHz, $CDCl_3$) δ 6.69 (t, J=7.2 Hz, 1H), 3.76 (s, 3H), 3.58 (s, 9H), 1.48–1.41 (m, 2H), 1.34 (sextet, J=7.3 Hz, 2H), 0.90 (t, J=7.2 Hz, 3H); ^{13}C NMR (100 MHz, $CDCl_3$) δ 169.0, 161.2, 125.5, 51.4, 50.9, 31.3, 22.4, 13.8; LRMS (ESI^+) m/z calcd for $(M+H)^+$ $[C_{11}H_{22}O_5Si]^+$: 263.1, found 263.1. *β-Isomer*: IR (film) 2954, 2844, 1727, 1194, 1089, 813 cm^{-1}; ^1H NMR (400 MHz, $CDCl_3$) δ 6.28 (s, 1H), 3.73 (s, 3H), 3.59 (s, 9H), 2.66 (t, J=7.8 Hz, 2H), 1.49–1.34 (comp. m, 4H), 0.93 (t, J=7.2 Hz, 3H); ^{13}C NMR (100 MHz, $CDCl_3$) δ 165.9, 155.4, 130.4, 51.4, 51.1, 31.6, 30.8, 23.4, 14.2; LRMS (ESI^+) m/z calcd for $(M+H)^+$ $[C_{11}H_{22}O_5Si]^+$: 263.1, found 263.1.

*4.2.9. Methyl (E)-2-(1,1,1,3,5,5,5-heptamethyltrisiloxan-3-yl)hept-2-enoate (**44**).* Hydrosilylation performed under air using Pt(dvds). Pale yellow oil. Yield 98%, >19:1 α/β. R_f=0.52 in 19:1 hexanes/Et_2O. IR (film) 2959, 1721, 1609, 1258, 1200, 1075 cm^{-1}; ^1H NMR (400 MHz, $CDCl_3$) δ 6.44 (t, J=7.2 Hz, 1H), 3.72 (s, 3H), 2.43 (q, J=7.3 Hz, 2H), 1.46–1.31 (comp. m, 2H), 0.92 (t, J=7.2 Hz, 3H), 0.18 (s, 3H), 0.10 (s, 18H); ^{13}C NMR (100 MHz, $CDCl_3$) δ 170.1, 156.1, 133.5, 51.0, 31.2, 31.2, 22.5, 14.0, 1.9, 0.3; HRMS (ESI^+) m/z calcd for $(M+H)^+$ $[C_{15}H_{35}O_4Si_3]^+$: 363.1838, found 363.1846.

*4.2.10. (E)-3-(Triethylsilyl)oct-3-en-1-yl acetate (**46**).* Hydrosilylation performed under Ar. Colorless oil. Yield 90%, 3.8:1 α/β. R_f=0.38 in 19:1 hexanes/Et_2O. (Data for α-isomer only.) IR (film) 2956, 1745, 1464, 1239, 1031, 718 cm^{-1}; ^1H NMR (400 MHz, $CDCl_3$) δ 5.81 (t, J=7.0 Hz, 1H), 3.95 (app. t, J=8.0 Hz, 2H), 2.44 (dd, J=8.3, 7.6 Hz, 2H), 2.17 (q, J=7.1 Hz, 2H), 2.05 (s, 3H), 1.39–1.33 (comp. m, 4H), 0.92 (t, J=7.8 Hz, 9H), 0.60 (q, J=7.8 Hz, 6H); ^{13}C NMR (100 MHz, $CDCl_3$) δ 171.5, 146.0, 132.1, 64.2, 32.3, 29.4, 28.9, 22.9, 21.5, 14.5, 7.8, 3.4; HRMS ($DART^+$) m/z calcd for $(M+NH_4)^+$ $[C_{16}H_{36}NO_2Si]^+$: 302.2515, found 302.2518.

*4.2.11. (E)-3-(Dimethyl(phenyl)silyl)oct-3-en-1-yl acetate (**47**).* Hydrosilylation performed under Ar. Colorless oil. Yield 93%, 3.1:1 α/β. R_f=0.53 in 9:1 hexanes/EtOAc. (Data for α-isomer only.) IR (film) 2958, 1743, 1241, 1110, 1033, 818 cm^{-1}; ^1H NMR (400 MHz, $CDCl_3$) δ 7.51–7.48 (m, 2H), 7.35–7.32 (comp. m, 3H), 5.96 (t, J=7.0 Hz, 1H), 3.86 (app. t, J=7.8 Hz, 2H), 2.45 (t, J=7.6 Hz, 2H), 2.18 (q, J=7.1 Hz, 2H), 1.97 (s, 3H), 1.39–1.31 (comp. m, 4H), 0.92 (t, J=7.1 Hz, 3H), 0.36 (s, 6H); ^{13}C NMR (100 MHz, $CDCl_3$) δ 171.3, 146.4, 138.9, 134.2, 133.6, 129.2, 128.0, 64.0, 32.0, 29.1, 29.0, 22.8, 21.3, 14.3, −2.5; HRMS ($APCI^+$) m/z calcd for $(M+NH_4)^+$ $[C_{18}H_{32}NO_2Si]^+$: 322.2202, found 322.2191.

*4.2.12. (E)-3-(Triphenylsilyl)oct-3-en-1-yl acetate (**48**).* Hydrosilylation performed under Ar. White solid. Yield 98%, 4.5:1 α/β. R_f=0.47 in 9:1 hexanes/EtOAc. (Data for α-isomer only.) IR (film) 3069, 2957, 1741, 1428, 1240, 702 cm^{-1}; ^1H NMR (400 MHz, $CDCl_3$) δ 7.56–7.54 (m, 6H), 7.43–7.35 (comp. m, 9H), 6.13 (t, J=7.0 Hz, 1H), 3.75 (t, J=7.6 Hz, 2H), 2.58 (t, J=7.6 Hz, 2H), 2.29 (q, J=7.1 Hz, 2H), 1.86 (s, 3H), 1.40–1.32 (comp. m, 4H), 0.91 (t, J=7.0 Hz, 3H); ^{13}C NMR (100 MHz, $CDCl_3$) δ 171.4, 151.4, 136.8, 134.8, 130.0, 128.3, 64.3, 32.1, 29.7, 23.1, 21.4, 14.5; HRMS ($APCI^+$) m/z calcd for $(M+NH_4)^+$ $[C_{28}H_{36}NO_2Si]^+$: 446.2515, found 446.2508.

*4.2.13. (E)-3-(Ethoxydimethylsilyl)oct-3-en-1-yl acetate (**49**).* Hydrosilylation performed under Ar. Colorless oil. Yield 94%, 3.9:1 α/β. R_f=0.31 in 9:1 hexanes/EtOAc. (Data for α-isomer only.) ^1H NMR (400 MHz, $CDCl_3$) δ 5.98 (t, J=6.9 Hz, 1H), 4.01 (t, J=7.8 Hz, 2H), 3.63 (q, J=7.0 Hz, 2H), 2.50 (t, J=7.8 Hz, 2H), 2.17 (q, J=7.1 Hz, 2H), 2.05 (s, 3H), 1.40–1.32 (comp. m, 4H), 1.19 (t, J=7.0 Hz, 3H), 0.92 (t, J=7.1 Hz, 3H), 0.20 (s, 6H); ^{13}C NMR (100 MHz, $CDCl_3$) δ 171.5, 146.3, 134.3, 64.2, 58.8, 32.0, 28.8, 28.7, 22.9, 21.5, 18.9, 14.5, −1.6; HRMS ($APCI^+$) m/z calcd for $(M+H)^+$ $[C_{14}H_{28}O_3Si]^+$: 273.1808, found 273.1800.

*4.2.14. (E)-3-(Triethoxysilyl)oct-3-en-1-yl acetate (**50**).* Hydrosilylation performed under Ar. Colorless oil. Yield 87%, 4.2:1 α/β. R_f=0.24 in 9:1 hexanes/Et_2O. (Data for α-isomer only.) IR (film) 2974, 1744, 1618, 1388, 1242, 959, 781 cm^{-1}; ^1H NMR (400 MHz, $CDCl_3$) δ 6.22 (t, J=7.0 Hz, 1H), 4.06 (t, J=7.6 Hz, 2H), 3.81 (q, J=7.6 Hz, 6H), 2.47 (t, J=7.3 Hz, 2H), 2.17 (q, J=7.2 Hz, 2H), 2.03 (s, 3H), 1.43–1.29 (comp. m, 4H), 1.22 (t, J=7.1 Hz, 9H), 0.91 (t, J=7.3 Hz, 3H); ^{13}C NMR (100 MHz, $CDCl_3$) δ 171.5, 149.4, 127.9, 64.1, 58.9, 31.8, 28.81, 28.77, 22.9, 21.5, 18.6, 14.4; HRMS (ESI^+) m/z calcd for $(M+Na)^+$ $[C_{16}H_{32}NaO_5Si]^+$: 355.1917, found 355.1906.

*4.2.15. (E)-3-(Trimethoxysilyl)oct-3-en-1-yl acetate (**51**).* Hydrosilylation performed under Ar. Colorless oil. Yield 88%, 3.2:1 α/β. R_f=0.31 in 9:1 hexanes/EtOAc. (Data for α-isomer only.) IR (film) 2958, 2842, 1744, 1617, 1243, 811 cm^{-1}; ^1H NMR (400 MHz, $CDCl_3$) δ 6.21 (t, J=7.1 Hz, 1H), 4.06 (t, J=7.5 Hz, 2H), 3.57 (s, 9H), 2.48 (t, J=7.5 Hz, 2H), 2.29 (q, J=7.1 Hz, 2H), 2.03 (s, 3H), 1.42–1.30 (comp. m, 4H), 0.92 (t, J=7.1 Hz, 3H); ^{13}C NMR (100 MHz, $CDCl_3$) δ 171.5, 150.1, 126.8, 64.1, 51.1, 31.8, 28.8, 21.7, 22.9, 21.5, 14.4; HRMS (ESI^+) m/z calcd for $(M+Na)^+$ $[C_{13}H_{26}O_5SiNa]^+$: 313.1447, found 313.1446.

Acknowledgements

Colorado State University is acknowledged for support of our research program. Eli Lilly and Company (_100004312) is gratefully acknowledged for a graduate research fellowship to D.A.R.

References and notes

1. (a) Marciniec, B. Hydrosilylation In *Advances in Silicon Science*; Marciniec, B., Ed.; Springer: Dordrecht, Netherlands, 2009, Chapters 1–2; (b) Trost, B. M.; Ball, Z. T. *Synthesis* **2005**, 853–887.
2. Jones, G. R.; Landais, Y. *Tetrahedron* **1996**, *52*, 7599–7662.
3. Curtis-Long, M. J.; Aye, Y. *Chem.—Eur. J.* **2009**, *15*, 5402–5416.
4. Denmark, S. E.; Liu, J. H.-C. *Angew. Chem., Int. Ed.* **2010**, *49*, 2978–2986.
5. Tamao, K.; Akita, M.; Maeda, K.; Kumada, M. *J. Org. Chem.* **1987**, *52*, 1100–1106.
6. Rooke, D. A.; Ferreira, E. M. *J. Am. Chem. Soc.* **2010**, *132*, 11926–11928.
7. Rooke, D. A.; Ferreira, E. M. *Angew. Chem., Int. Ed.* **2012**, *51*, 3225–3230.
8. Kopping, B.; Chatgilialoglu, C.; Zehnder, M.; Giese, B. *J. Org. Chem.* **1992**, *57*, 3994–4000.
9. Sudo, T.; Asao, N.; Yamamoto, Y. *J. Org. Chem.* **2000**, *65*, 8919–8923.
10. Takahashi, T.; Bao, F.; Gao, G.; Ogasawara, M. *Org. Lett.* **2003**, *5*, 3479–3481.
11. Molander, G. A.; Knight, E. E. *J. Org. Chem.* **1998**, *63*, 7009–7012.
12. (a) Jun, C. H.; Crabtree, R. H. *J. Organomet. Chem.* **1993**, *447*, 177–187; (b) Ojima, I.; Clos, N.; Donovan, R. J.; Ingallina, P. *Organometallics* **1990**, *9*, 3127–3133.
13. Trost, B. M.; Ball, Z. T. *J. Am. Chem. Soc.* **2005**, *127*, 17644–17655.
14. Chalk, A. J.; Harrod, J. F. *J. Am. Chem. Soc.* **1965**, *87*, 16–21.
15. (a) Speier, J. L.; Webster, J. A.; Barnes, G. A. *J. Am. Chem. Soc.* **1957**, *79*, 974–979; (b) Their report was disclosed subsequent to a patent by Wagner using Pt/C a few months earlier. Wagner, G. H.; Strother, C. O. U.S. Patent 2,632,013, Mar. 17, 1953.
16. Steffanut, P.; Osborn, J. A.; DeCian, A.; Fisher, J. *Chem.—Eur. J.* **1998**, *4*, 2008–2017.
17. Roy, A. K.; Taylor, R. B. *J. Am. Chem. Soc.* **2002**, *124*, 9510–9524.
18. Berthon-Gelloz, G.; Schumers, J.-M.; De Bo, G.; Markó, I. E. *J. Org. Chem.* **2008**, *73*, 4190–4197.
19. (a) McLaughlin, M. G.; Cook, M. J. *Chem. Commun.* **2011**, 11104–11106; (b) McAdam, C. A.; McLaughlin, M. G.; Johnston, A. J. S.; Chen, J.; Walter, M. W.; Cook, M. J. *Org. Biomol. Chem.* **2013**, *11*, 4488–4502.
20. Sumida, Y.; Kato, T.; Yoshida, S.; Hosoya, T. *Org. Lett.* **2012**, *14*, 1552–1555.
21. (a) Stork, G.; Jung, M. E.; Colvin, E.; Noel, Y. *J. Am. Chem. Soc.* **1974**, *96*, 3684–3686; (b) Thorimbert, S.; Malacria, M. *Tetrahedron Lett.* **1996**, *37*, 8483–8486; (c) Li, J.; Suh, J. M.; Chin, E. *Org. Lett.* **2010**, *12*, 4712–4715.
22. Tsipis, C. A. *J. Organomet. Chem.* **1980**, *187*, 427–446.
23. Dorman, D. E.; Jautelat, M.; Roberts, J. D. *J. Org. Chem.* **1973**, *38*, 1026–1030.
24. (a) Hamze, A.; Provot, O.; Alami, M.; Brion, J.-D. *Org. Lett.* **2005**, *7*, 5625–5628; (b) Hamze, A.; Provot, O.; Brion, J.-D.; Alami, M. *Synthesis* **2007**, 2025–2036.
25. In this and all cases of the Pt-catalyzed hydrosilylations evaluated, we only observed (*E*)-selectivity. No (*Z*)-isomers were observed.
26. We attribute this efficiency largely to the increased solubility of the Pt catalyst in CH_2Cl_2.
27. Of note, 1 mol % Karstedt's catalyst was employed due to the fact that it is a 3 wt % solution in PDMS and removing large amounts of PDMS can be quite cumbersome.
28. We did find that reactions would not proceed to completion with lower catalyst loadings.
29. Chang, W. T.; Smith, R. C.; Regens, C. S.; Bailey, A. D.; Werner, N. S.; Denmark, S. E. *Org. React.* **2011**, *75*, 213–745.

30. For examples of the use of this reagent in Pt catalyzed hydrosilylations of terminal alkynes, see: (a) Hamze, A.; Provot, O.; Brion, J.-D.; Alami, M. *J. Organomet. Chem.* **2008**, *693*, 2789–2797; (b) Sonnek, G.; Drahs, E.; Jancke, H.; Hamann, H. *J. Organomet. Chem.* **1990**, *386*, 29–35.
31. Rooke, D. A.; Ferreira, E. M. *Org. Lett.* **2012**, *14*, 3328–3331.
32. Kawasaki, Y.; Ishikawa, Y.; Igawa, K.; Tomooka, K. *J. Am. Chem. Soc.* **2011**, *133*, 20712–20715.
33. (a) The regioselectivities observed here are quite different than those in Cook's studies of propargylic alcohols. We attribute this difference to his use of a bulky XPhos ligand in conjunction with a Pt catalyst. See Ref. 19. (b) Cook invoked hydrogen bonding between the alcohol hydrogen and the platinum *hydride*. Although we do not eliminate that as a possibility, we do not prefer that interaction in our case, as we observe hydride delivery to the alkyne β-carbon.
34. Matsumoto, H.; Hoshino, Y.; Nagai, Y. *Chem. Lett.* **1982**, 1663–1666.
35. Alami, M.; Liron, F.; Gervais, M.; Peyrat, J.-F.; Brion, J.-D. *Angew. Chem., Int. Ed.* **2002**, *41*, 1578–1580.
36. Rubin, M.; Trofimov, A.; Gevorgyan, V. *J. Am. Chem. Soc.* **2005**, *127*, 10243–10249.
37. For other elegant examples of the application of this correlation, see: (a) Hydroalumination: Igawa, K.; Tomooka, K. *Angew. Chem., Int. Ed.* **2006**, *45*, 232–234; (b) Au- and Zn-catalyzed hydroxyanilide addition: Wang, Y.; Liu, L.; Zhang, L. *Chem. Sci.* **2013**, *4*, 739–746.